Development of Molecular Probes for the Identification of Extra Interaction Sites in the Mid-Gorge and Peripheral Sites of Butyrylcholinesterase (BuChE). Rational Design of Novel, Selective, and Highly Potent BuChE Inhibitors[†]

Giuseppe Campiani,*,[‡,§] Caterina Fattorusso,[§,||] Stefania Butini,[‡,§] Alessandra Gaeta,[‡,§] Marianna Agnusdei,[‡,§] Sandra Gemma,[‡,§] Marco Persico,[§,||] Bruno Catalanotti,[§,||] Luisa Savini,[‡,§] Vito Nacci,[‡,§] Ettore Novellino,[§,||] Harold W. Holloway,[⊥] Nigel H. Greig,[⊥] Tatyana Belinskaya,[#] James M. Fedorko,[#] and Ashima Saxena[#]

Dipartimento Farmaco Chimico Tecnologico, via Aldo Moro, and European Research Centre for Drug Discovery and Development (NatSynDrugs), Università di Siena, 53100 Siena, Italy, Dipartimento di Chimica delle Sostanze Naturali e Dipartimento di Chimica Farmaceutica e Tossicologica Università di Napoli Federico II, via D. Montesano 49, 80131 Napoli, Italy, Drug Design & Development Section, Intramural Research Program National Institute of Aging, NIH, Baltimore, Maryland 21224, and Division of Biochemistry, Walter Reed Army Institute of Research, Silver Spring, Maryland 20910

Tacrine heterobivalent ligands were designed as novel and reversible inhibitors of cholinesterases. On the basis of the investigation of the active site gorge topology of butyrylcholinesterase (BuChE) and acetylcholinesterase (AChE) and by using flexible docking procedures, molecular modeling studies formulated the hypothesis of extra interaction sites in the active gorge of hBuChE, namely, a mid-gorge interaction site and a peripheral interaction site. The design strategy led to novel BuChE inhibitors, balancing potency and selectivity. Among the compounds identified, the heterobivalent ligand **4m**, containing an amide nitrogen and a sulfur atom at the 8-membered tether level, is one of the most potent and selective BuChE inhibitors described to date. The novel inhibitors, bearing postulated key features, validated the hypothesis of the presence of extra interaction sites within the hBuChE active site gorge.

Introduction

Alzheimer's disease (AD) is the leading cause of dementia among older people. An estimated 10% of the world's population over the age of 65 and a half of that over the age of 85 are afflicted by AD. With the graying of the European, North American, and Asian population, AD is expected to reach epidemic proportions over the next two decades, which makes the development of new therapeutic strategies and effective drugs essential.

Numerous studies have highlighted that the cholinergic neurotransmission system is profoundly compromised in the AD brain, with losses of cholinergic neurons and synapses occurring in the forebrain, cortex, and hippocampus. The efficacy of cholinergic therapies in AD supports the cholinergic hypothesis and validates this neurotransmitter system as a therapeutic target.[1] Among the various restorative strategies explored, the use of reversible inhibitors of AChE (AChEIs) is considered to be a viable and attractive therapeutic approach to amplify the action of the residual acetylcholine (ACh) in the brain of AD patients.[2] In this regard, four AChEIs have been approved by the European and U.S. regulatory authorities and are commonly prescribed: tacrine (**1**) (1993, Cognex), donepezil (1996, Aricept), rivastigmine (2000, Exelon), and galantamine (2001, Reminyl). Although these drugs augment cognition and

may impact the disease course to prevent or slow further memory loss, they are often associated with adverse events (e.g., liver damage, nausea, and vomiting) and their therapeutic potential is limited.

Although the forebrain cholinergic system is clearly perturbed during mild to moderate AD, by the time the disease has progressed to its severe stage, AChE and choline acetyltransferase levels are as much as 85−90% lower than normal. Interestingly, this loss of AChE is accompanied by an increase in BuChE levels by up to 2-fold.[2] Although 50−60% homologous, these enzymes are encoded by different genes and clearly differ in substrate specificity and sensitivity to inhibitors, likely due mainly to a larger void and/or to structural differences in the active site gorge of BuChE.[3,4]

AChE and BuChE both hydrolyze ACh, albeit with slightly different kinetics, and coexist ubiquitously in humans.[1] BuChE is widely distributed in the body of vertebrates. It appears in serum, liver, lung, and heart and within the CNS; in particular, in normal brain some 10−15% of cholinergic neurons possess BuChE, rather than AChE, as their metabolizing enzyme, and BuChE is often expressed and secreted by glyal cells.[1,5] These latter are elevated in the AD brain, accounting for the increased expression of BuChE. Hence, the depletion of AChE and elevation of BuChE in the AD brain causes a mismatching between ACh synthesis/synaptic release and its enzymatic hydrolysis, suggesting that BuChE inhibition may provide therapeutic value in moderate and severe disease.

Unlike AChE, the physiologic function of BuChE in normal and diseased humans remains unclear, although a role in neurodegenerative disorders has been sug-

* To whom correspondence should be addressed. Tel: 0039-0577-234172. Fax: 0039-0577-234333. E-mail: campiani@unisi.it.
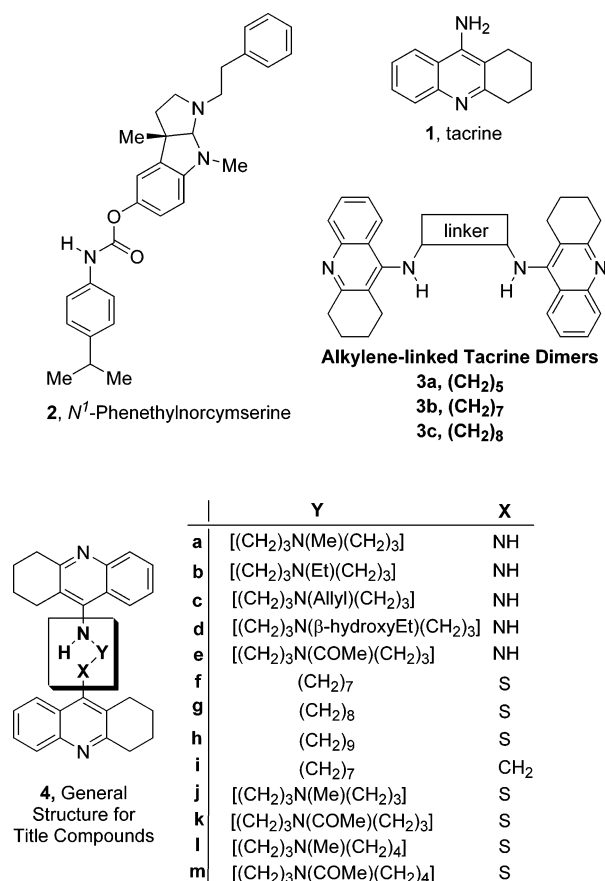† In memory of Dr. Paul Janssen.
‡ Università degli Studi di Siena.
§ European Research Centre for Drug Discovery and Development (NatSynDrugs).
|| Università degli Studi di Napoli "Federico II".
⊥ National Institute of Aging.
Walter Reed Army Institute of Research.

Chart 1

Scheme 1[a]

[a] Reagents: (i) dry CH_3CN, R–X (X = Br, I), K_2CO_3, room temperature, 12 h; (ii) dry dichloromethane, CF_3CO_2H, room temperature, 1 h; (iii) 9-chloro-1,2,3,4-tetrahydroacridine, pentanol, TEA, 160 °C, 12 h; (iv) dry CH_3CN, KOH, $TsO(CH_2)_9OTs$, room temperature, 12 h; (v) 9-mercapto-1,2,3,4-tetrahydroacridine, dry CH_3CN, KOH, room temperature, 4 h.
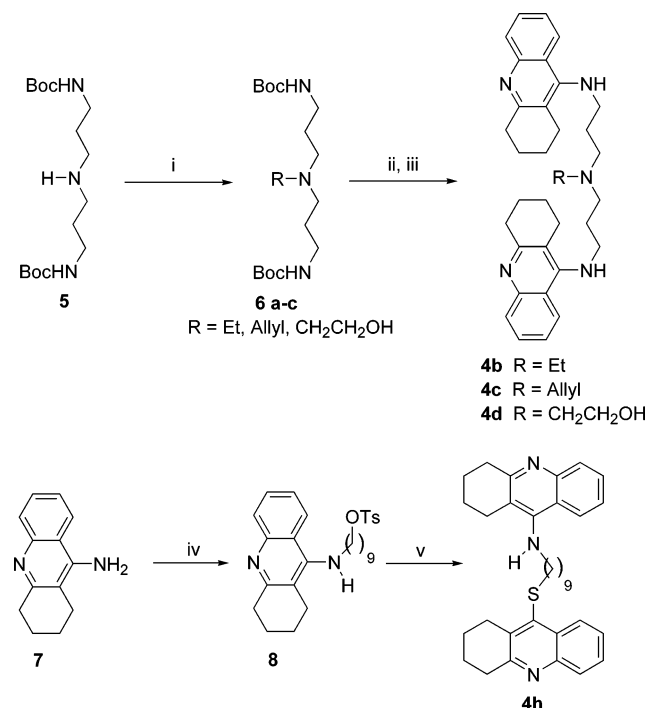
gested. Ongoing elucidation of the properties and behavior of BuChE in normal and AD brains supports a role for BuChE in AD pathology as well as normal cognition.[6] Indeed, the survival of AChE knockout mice with normal levels and localization of BuChE[7] supports the concept that BuChE can partly compensate for AChE action. The additional demonstration that central BuChE rather than AChE inhibition is the best correlate of cognitive improvement in AD clinical studies with the dual ChEI rivastigmine (Exelon)[9] further suggests that BuChE represents an intriguing target to develop drugs for the treatment of neurodegenerative diseases. By consequence, the availability of specific bivalent ligands targeting this enzyme would be crucial to evaluate its therapeutic value. However, drugs with high affinity for BuChE together with a significant inhibitory activity on AChE would also represent a valuable therapeutic approach for use in mild, moderate, and severe dementia.

Few BuChEIs have been reported to date, the most interesting ones being structurally related to phenserine and represented by **2**.[8] Recently, the existence of a peripheral site at the lip of the gorge of equine and human BuChEs was hypothesized using molecular docking techniques, and a series of tacrine-based heterobivalent ligands (HBLs) was developed.[10,11]

The aim of the present study was the development of novel tacrine-based HBLs for pharmacological evaluation against BuChE, in order to provide molecular probes to gain further insights into the active site gorge of BuChE, as well as to develop novel potential AD therapeutics.

Based on a molecular modeling approach, a series of new ligands (**4**) was designed and tested (Chart 1). The new subset of ChEIs reported herein showed increased potency and selectivity, thus confirming the predicted accessibility to different interaction sites in the BuChE active site at the mid and peripheral gorge level. These compounds represent the second generation of BuChEIs.

Chemistry

Compounds **4a** and **4e,f** were obtained as previously reported,[11] and the synthetic pathways to obtain compounds **4b−d** and **4h−m** are described in Schemes 1−3. Scheme 1 represents the synthesis of derivatives **4b−d,h**. N-Alkylation of the protected amine **5**, in turn prepared from the commercially available triamine by a standard method, with the appropriate alkylating agent gave the intermediate amines **6a−c** in good yields. These, after deprotection, were treated with 9-chloro-1,2,3,4-tetrahydroacridine to provide the desired compounds **4b−d**. The analogue **4h** was obtained starting from commercially available tacrine (**7**), which was N-alkylated to give compound **8**, which, after treatment with 1,2,3,4-tetrahydro-9-thioacridine (**15**),[11] furnished **4h** in good yield. To obtain **4i**, as represented in Scheme 2, we used the ester **10**, which was in turn prepared starting from the commercially available acid **9** by treatment with diazomethane. Thereafter, the reduction of the ester **10**, accomplished by means of DIBAL-H, gave the aldehyde **11**, which underwent a Wittig reaction with 6-cyanohexyl-1-triphenylphosphonium bromide to give the olefin **12**. Then, the amine **13**, obtained by reduction of the cyano group of **12** by means of $LiAlH_4$, was N-alkylated with 9-chloro-1,2,3,4-tet-

Scheme 2[a]
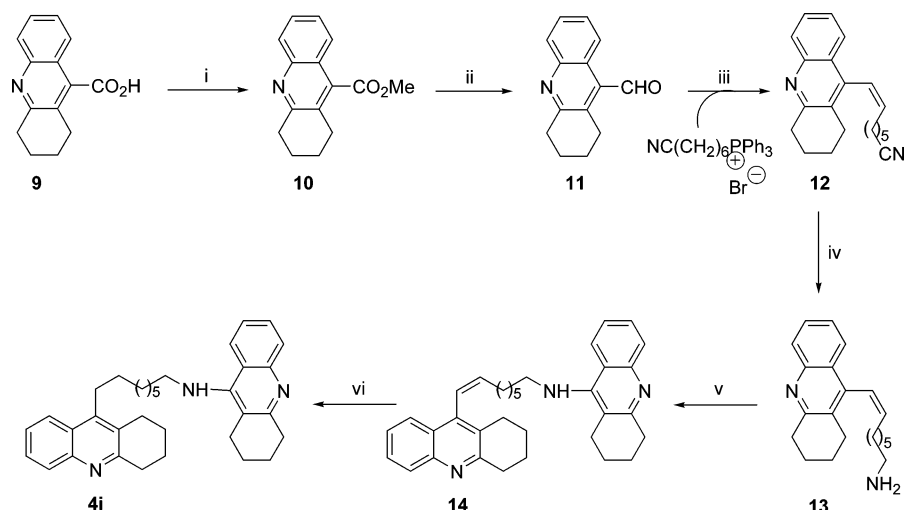
[a] Reagents: (i) diazomethane, methanol, room temperature, 2 h; (ii) (a) dry toluene, −78 °C, DIBAL-H, 2 h; (b) Rochelle salt, 2 h; (iii) (a) 6-cyanohexyl-1-triphenylphosphonium bromide, t-BuOK, dry THF, −78 °C; (b) **11**, room temperature, 1 h; (iv) LiAlH₄, dry Et₂O, room temperature, 2 h; (v) 9-chloro-1,2,3,4-tetrahydroacridine, pentanol, 160 °C, 12 h; (vi) H₂, Pd/C, methanol, 40 psi, 4 h.

Scheme 3[a]
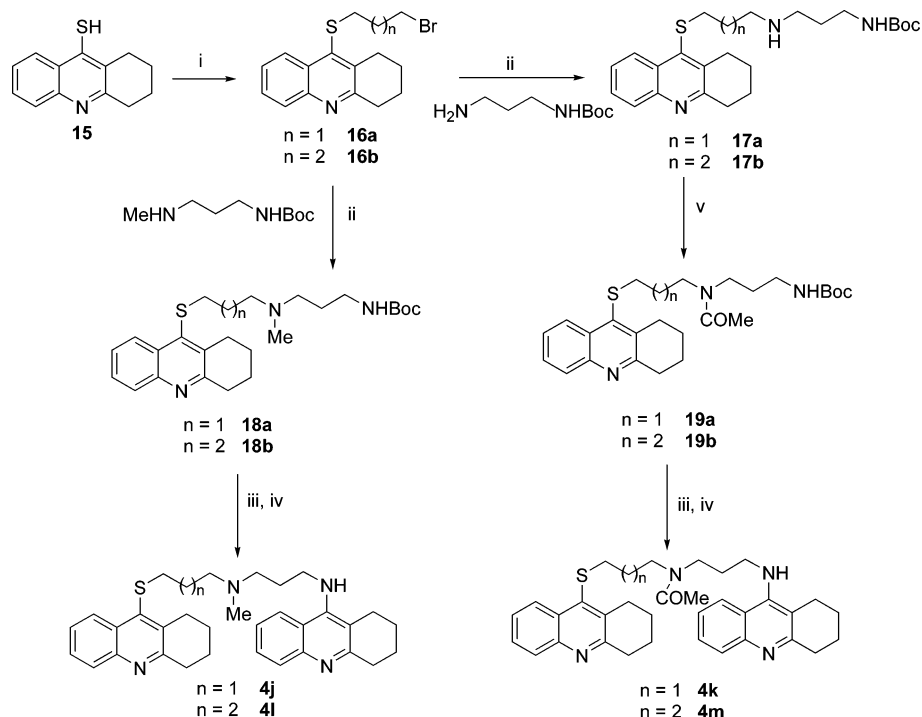
[a] Reagents: (i) 1,3-dibromobutane/1,3-dibromopropane, KOH, dry CH₃CN, room temperature, 12 h; (ii) dry CH₃CN, DIPEA, room temperature, 12 h; (iii) dry dichloromethane, CF₃COOH, room temperature, 1 h; (iv) 9-chlorotetrahydroacridine, dry CH₃CN, TEA, reflux, 12 h; (v) acetyl chloride, TEA, dry dichloromethane, room temperature, 3 h.

rahydroacridine to afford compound **14**, which was subjected to catalytic hydrogenation to give **4i**. According to Scheme 3, compounds **4j,k** were obtained starting from 1,2,3,4-tetrahydro-9-thioacridine **15**, which was treated with 1,3-dibromopropane or 1,4-dibromobutane to give compounds **16a,b**, which were then used as alkylating agents to provide compounds **18a,b** and **17a,b**. Derivatives **18a,b**, after deprotection and N-alkylation with 9-chloro-1,2,3,4-tetrahydroacridine gave the desired final compounds **4j** and **4l**. On the other hand, compounds **17a,b** were N-acylated by means of acetyl chloride, and the protected amines **19a,b** were used as starting material to obtain compounds **4k** and **4m**, as previously described for **18a,b**.

Results and Discussion

The Design of Novel Selective Inhibitors and Their Structure−Activity Relationships. Our rational approach started[10] with a thorough investigation of the topology of the active site gorges of AChEs and BuChEs, followed by a structural and pharmacological evaluation of three compounds (**3a−c**) devoloped by Carlier et al.[12] Altough **3a−c** were claimed as selective AChEIs (low affinity for rat BuChE), in our pharmacological assays they were found to be almost equally active against fetal bovine serum AChE (FBSAChE) and equine BuChE (EqBuChE). The different affinity of **3a−c** for EqBuChE and rat BuChE was explained by

Table 1. Dissociation Constants for the Inhibition of Fetal Bovine Serum (FBS) AChE and Equine (Eq) BuChE by Tacrine-Related Dimers

compd	tether length (atoms)n	FBSAChE^a K_i (nM)	EqBuChE^a K_i (nM)	AChE/ BuChE ratio
1^b		40	7	
3a	5	210 ± 13	100 ± 11	2.1
3b^b	7	1.3	2	0.65
3c	8	1.9 ± 0.3	2.0 ± 0.8	0.96
4a	7	0.06^b	6^b	0.01
4b	7	2.8 ± 0.6	0.94 ± 0.2	2.9
4c	7	1.6 ± 0.4	0.76 ± 0.05	2.1
4d	7	0.65 ± 0.1	3.3 ± 0.3	0.2
4e	7	1500^b	2^b	750
4f	7	340^b	35^b	9.7
4g	8	250^b	0.4^b	625
4h	9	195 ± 12	2.3 ± 0.1	86
4i	7	30 ± 3.4	27 ± 1.0	1.1
4j	7	9.1 ± 1.0	4.2 ± 0.8	2.2
4k	7	50 ± 6	0.23 ± 0.04	217
4l	8	130 ± 20	0.68 ± 0.02	191
4m	8	47 ± 4	0.11 ± 0.05	427
E2020^b		2.9	640	
Etho^{b,c}		173200	20	

^{a} K_i is the mean of at least three determinations. ^{b} From ref 9. ^{c} Ethopropazine. **1**, tacrine; **3b**, tacrine homodimer (7 methylenes).

Table 2. Inhibition of Human AChE and Human BuChE (IC$_{50}$, nM) by a Selected Set of Tacrine-Related Dimers

compd	tether length (atoms)n	hAChE^a	hBuChE^a
4a	7	0.30 ± 0.05	10.4 ± 0.4
4b	7		3.4 ± 0.6
4e	7		3.9 ± 0.2
4g	8		0.77 ± 0.19

^{a} IC$_{50}$ is the mean of at least three determinations.

the significant differences between the amino acid composition at the lip of the gorge of the two enzymes (Ala/Val/Lys in human, equine, and rat BuChE, respectively).[10]

Exploiting the different physical−chemical properties related to the different amino acid composition of the active site gorges of the two classes of enzymes, we rationally modified the tacrine homobivalent structure of **3b** to obtain ChEIs with specific potency and selectivity, according to the results of our flexible docking studies.[10,11] This approach led to the hypothesis of the presence of an AChE mid-gorge recognition site, demonstrated by the development of potent AChE ligands capable to bind the three established interaction points.[11] Moreover, we also investigated the role played by cation−π and hydrophobic interactions in the binding of BuChEs, hypothesizing (i) that the lack of a protonatable amino group on one unit of the ligand could be partially compensated by a high degree of hydrophobicity and (ii) the existence of a peripheral interaction site on BuChEs (hBuChE F278).[10,11]

On these bases, we herein report the development of novel BuChEIs with balanced potency and selectivity able to bind novel and specific sites of interaction along the enzyme gorge.

Molecular modeling studies were performed using human enzymes, since they represent the pharmacological target for the development of new drugs, although our pharmacological tests used FBSAChE and EqBuChE. Nevertheless, a comparison of their amino acid sequences with those of the corresponding human enzymes revealed an overall identity of 84% and 88%, respectively. Only small differences were found comparing the amino acid composition of the active sites (residues within 5 Å from any atom of HBLs) of FBSAChE/hAChE, and hBuChE/EqBuChE. Biological results on human enzymes are shown on a limited set of compounds (Table 2) and seem to support our modeling studies, at least as far as affinity on human BuChE is concerned.

Selected conformers of compounds **4d**, **4e**, **4g**, **4k**, **4l**, and **4m** were docked into the hAChE X-ray structure (PDB code 1B41), and into the hBuChE X-ray structure recently solved by Juan Fontecilla-Camps and co-workers (PDB code 1P0I) using a protocol which included molecular mechanics, Monte Carlo, and simulated annealing calculations.

Our results showed (Table 1) that AChE/BuChE potency and selectivity of ChEIs can be dramatically affected by the introduction of a nitrogen atom bearing different chemical groups in the middle of the HBL alkyl tether, with the potential to establish extra interactions in the mid-gorge region. Indeed, AChE/BuChE selectivity is reversed if the basic nitrogen of the tether of **4a** ($K_{i(FBSAChE)}$ = 0.06 nM, $K_{i(EqBuChE)}$ = 6.0 nM)[11] (IC$_{50(hAChE)}$ = 0.30 nM; IC$_{50(hBuChE)}$ = 10.4 nM) is replaced by the neutral, bulkier amide group as in compound **4e** ($K_{i(FBSAChE)}$ = 1500 nM; $K_{i(EqBuChE)}$ = 2.0 nM)[11] (IC$_{50(hBuChE)}$ = 3.90 nM), according to the different chemical environment at the gorge level of the two enzymes. Starting from our lead **4a**, we attempted to modulate AChE/BuChE potency and selectivity by introducing different alkyl chains at the tether nitrogen. In agreement with the larger void at the BuChE active site gorge, an increase in the bulk of the alkyl chain resulted in a decrease in affinity for FBSAChE and an increase in affinity for EqBuChE (**4a** vs **4b**−**d**). Accordingly, the *N*-ethyl derivative **4b** showed a K_i of 2.84 nM and 0.94 nM for FBSAChE and EqBuChE, respectively, and its analogue **4c**, bearing an allyl chain, showed a K_i of 1.60 nM and 0.76 nM for FBSAChE and EqBuChE, respectively. Following a different trend, compound **4d**, bearing a β-hydroxyethyl chain at the nitrogen level, was found more potent for FBSAChE ($K_{i(FBSAChE)}$ = 0.65 nM, $K_{i(EqBuChE)}$ = 3.30 nM) compared to **4b** (Et) and **4c** (allyl), but still 10 times less potent than **4a**. The behavior of **4d** was explained by docking studies with hAChE (Figure 1A). The possibility to establish an extra water-mediated hydrogen bonding between the hydroxyl group of **4d** and the phenol OH group of Y124 of hAChE may explain its higher affinity with respect to **4b** and **4c**; on the other hand, its lower AChE affinity, in comparison with **4a**, may be due to the weakening of the electrostatic (cation−π) interactions with aromatic residues at the mid-gorge level, resulting from the presence of the bulkier β-hydroxyethyl chain, and to a weaker π−π stacking interaction with W86 at the catalytic site (Figure 1A).

4g was specifically designed hypothesizing that an 8-methylene linker would be optimal for π−π interaction between the *S*-tetrahydroacridine moiety and F278 at the peripheral site of BuChE (Figure 2A). Accordingly, **4g** resulted in a 20-fold increase in inhibitory activity ($K_{i(FBSAChE)}$ = 250 nM, $K_{i(EqBuChE)}$ = 0.4 nM)[11] (IC$_{50(hBuChE)}$ = 0.77 nM), compared to **4f** (Table 1). To confirm that
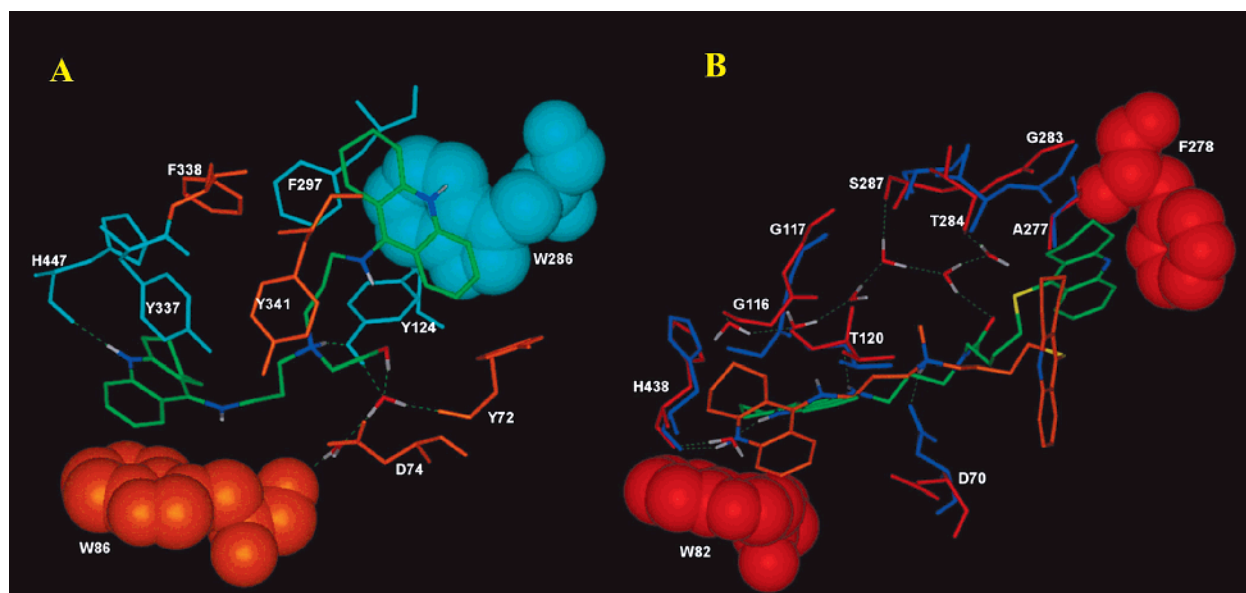
Figure 1. (A) Compound **4d** docked into the active site of hAChE. Conserved amino acids are colored in orange, and those replaced in hBuChE are colored in cyan. van der Waals volumes of W86 and W286 are displayed. (B) Docked complexes of **4l/**hBuChE (ligand, orange; protein, blue) and **4m/**hBuChE (ligand, green; protein, red; water molecules, by atom type), superimposed on Cα atoms. van der Waals volumes of W82 and F278 of **4m/**hBuChE complex are displayed. Hydrogen bonds are highlighted by green dashed lines. Hydrogens and water molecules are omitted for the sake of clarity, with the exception of those involved in hydrogen bond interactions.

Figure 2. Compounds **4g** (A) and **4k** (B) docked into the active site of hBuChE. Conserved amino acids are colored in cyan, and those replaced in hAChE and EqBuChE are colored in orange and white, respectively. van der Waals volumes of W82 and F278 are displayed. Hydrogen bonds are highlighted by green dashed lines. Hydrogens and water molecules are omitted for the sake of clarity, with the exception of those involved in hydrogen bond interactions.
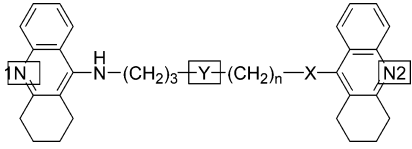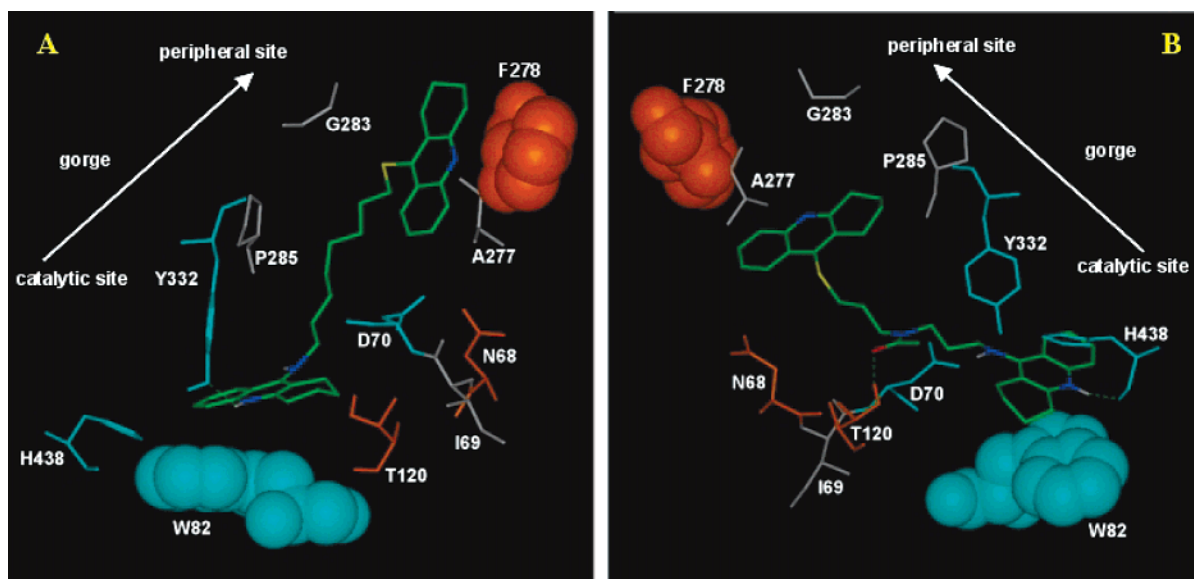
the 8-methylene tether was optimal for interaction with both sites, and to prove that the HBL **4g** is the prototypic compound for a second generation BuChEIs (two-point-interaction ligands, binding to the catalytic and the peripheral sites), we synthesized **4h**. The affinity of **4h** (9-methylene tether) for both enzymes was compared to **4g** (8-methylene tether) and **4f** (7-methylene tether) (Table 1). Whereas **4f** showed a lower affinity for EqBuChE (K_i = 35 nM),[11] compound **4h** showed a nanomolar affinity and high selectivity for EqBuChE ($K_{i(EqBuChE)}$ = 2.3 nM, Table 1) being 6 times less potent than **4g**, thus confirming the importance of an 8-methylene tether for interaction with the BuChE peripheral site (Figure 2A). Replacement of the sulfur atom in **4f**

by a methylene group (**4i**) significantly increased the affinity for FBSAChE, maintaining a nanomolar affinity for EqBuChE ($K_{i(FBSAChE)}$ = 30 nM, $K_{i(EqBuChE)}$ = 27 nM). As can be deduced from Tables 1 and 3, the affinity for FBSAChE of the 7-methylene-tethered ChEIs (characterized by an optimal interaction with the AChE peripheral anionic site W286) decreases dramatically in accordance with the lowering of the calculated protonatability of N2 (**4f** < **4i** < **3b**, Table 3). Indeed, docking studies with HBLs indicated that the most basic tacrine moiety is preferentially positioned at the catalytic site, according to the calculated electronegative gradient along the active site gorge of ChEs. By consequence, the pK_a value of the second tetrahydroacridine moiety of

Table 3. Calculated pK_a Values for Compounds **3b** and **4a**−**m**

				pK_a[a]			% mono-prot	% di-prot	% tri-prot
compd	Y	n	X	N1	Y	N2			
3b	CH$_2$	3	NH	9.40		8.80	2.43	97.55	
4a	N(Me)	3	NH	9.41	9.17	8.62	0.04	3.62	96.34
4b	N(Et)	3	NH	9.35	9.21	8.61	0.04	3.71	96.25
4c	N(allyl)	3	NH	9.35	8.25	8.74	0.23	7.95	91.82
4d	N(β-hydroxyEt)	3	NH	9.38	8.25	8.77	0.21	7.96	91.82
4e	N(COMe)	3	NH	9.33		8.73	2.85	97.13	
4f	CH$_2$	3	S	9.10		6.03	92.30	6.54	
4g	CH$_2$	4	S	9.10		6.03	92.30	6.54	
4h	CH$_2$	5	S	9.10		6.03	92.30	6.54	
4i	CH$_2$	3	CH$_2$	9.10		6.83	69.06	30.07	
4j	N(Me)	3	S	9.11	8.92	5.87	1.76	93.46	4.76
4k	N(COMe)	3	S	9.03		5.96	92.96	5.66	
4l	N(Me)	4	S	8.92	9.32	5.97	1.75	92.57	5.66
4m	N(COMe)	4	S	9.03		6.01	92.96	5.66	

[a] Apparent pK_a values calculated by using ACD/pK_a DB 7.0 software. (Advanced Chemistry Development Inc., Toronto, Canada).

HBLs (Table 3) is crucial for interaction at the peripheral site, thus affecting affinity and selectivity of ChEIs, according to the differences in amino acid residues at the gorge of the two enzymes. On this basis, with the specific aim of increasing BuChE potency and selectivity by lowering the protonatability of the aromatic N2 nitrogen (Table 3), one tacrine moiety of **4a** and **4e** was replaced by an *S*-tetrahydroacridine system (**4j** and **4k**, respectively). As expected, the affinity of **4j** and **4k** for EqBuChE increased to 4.2 nM and 0.23 nM, respectively. It is noteworthy that **4k**, characterized by the presence of a neutral amide group at the tether level, and an *S*-tetrahydroacridine moiety, is a potent and selective BuChEI, with an AChE/BuChE ratio of 217. Docking of compound **4k** in the hBuChE X-ray structure showed that the tacrine moiety still interacts with the catalytic site through a $\pi-\pi$ interaction with W82 and a H-bond with the backbone of H438 (Figure 2B). The amide function in the linker is H-bonded with the hydroxyl hydrogen of T120. No $\pi-\pi$ interaction with F278 was detectable at the lip of the gorge, due to the presence of the 7-membered tether (**4k** vs **4g**, Figure 2A,B). To further improve BuChE potency and selectivity, starting from **4j**, we designed compound **4l**, which combines the effect of the BuChE optimal tether length (8 methylenes) with the tetrahydrothioacridine system. Investigation of the binding mode of **4l** in hBuChE crystal structure by docking studies (Figure 1B) indicated that (i) the tacrine moiety of **4l** interacts with W82 and H438 at the catalytic site through a polarized $\pi-\pi$ interaction and a H-bond, respectively, and (ii) the protonated amine function of the linker interacts with the mid-gorge D70 by the way of a charge assisted H-bond. Despite the presence of the optimal 8-membered tether for binding either the catalytic or the peripheral site, no interaction at the lip of the gorge was observed for **4l**. A detailed analysis of the results of docking studies (Figure 1B) suggested that **4l** is "constrained" by the strong ionic interaction with D70, thereby compromising the interaction of the tetrahydrothioacridine moiety with F278. The inhibitory profile of **4l** (EqBuChE K_i = 0.68 nM; FBSAChE K_i = 130 nM)

confirmed our hypothesis on the presence of a mid-gorge interaction point in BuChEs. Its profile is very similar to **4g**, a two-point interaction BuChE ligand which interacts with both the catalytic and peripheral sites (F278). The lower AChE/BuChE affinity ratio of **4l** vs **4g** is due to the presence of the charged nitrogen at the tether level. Accordingly, we designed **4m**, in which the optimal length of the tether (8 atoms) was combined with an amide function and a tetrahydrothioacridine moiety. **4m** proved to be one of the most potent and selective BuChE inhibitors described to date. Docking of **4m** into the hBuChE X-ray structure showed that this compound is able to interact with both the catalytic and peripheral sites, with an additional binding at the mid-gorge level ($K_{i(EqBuChE)}$ = 0.11 nM) (Figure 1B). Comparison of the docked complexes of **4l**/hBuChE and **4m**/hBuChE (Figure 1B) highlighted a noteworthy aspect of the side chain of D70, reflecting the different basicity (pK_a value, Table 3) of the nitrogen atoms at the tether level. Moreover, the **4m**/hBuChE docked complex shows that the tacrine moiety in the catalytic site is shifted toward the gorge, weakening the $\pi-\pi$ interaction with W82 and interacting with the carbonyl group of H438 through a water mediated H-bond (Figure 1B). At the gorge level, the amide function of the tether binds a water molecule involved in a H-bond network with the protein. At the lip of the gorge, the tetrahydrothioacridine moiety gives a face-to-edge polarized $\pi-\pi$ interaction with F278. Enzymatic assays on this compound confirmed an increased affinity toward BuChE compared to **4g** (**4m**, EqBuChE K_i = 0.11 nM vs **4g**, EqBuChE K_i = 0.4 nM) with an AChE/BuChE affinity ratio of 427.

Conclusions

In summary, we disclosed the rational design of a novel series of potent tacrine-based HBLs as second generation BuChE inhibitors, binding two or three interaction sites at the BuChE gorge level. Molecular modeling studies led to the identification of extra interaction sites in the mid-gorge and peripheral regions of BuChE, leading to the design of the picomolar affinity ligands **4b,c,g,k,l,m**. The biological data were in full agreement with the proposed binding mode, confirming our hypothesis.

Of the few molecules reported in the literature that specifically interact with BuChE, compounds **4k**, **4l**, and **4m** represent three of the most potent and selective inhibitors described to date, and may prove to be useful pharmacological tools to investigate the physiological role of BuChE in health, development, aging, and disease. In particular, the biological data of **4k,l** confirmed the existence of an unprecedentedly described BuChE mid-gorge binding region.

4m, a novel three point interaction BuChE ligand binding to the catalytic and the newly discovered mid-gorge and peripheral sites represents the most potent HBL of the series ($K_{i(EqBuChE)}$ = 0.11 nM, AChE/BuChE affinity ratio = 427).

Furthermore, HBLs **4g** and **4m**, interacting with F278 at the lip of the gorge of BuChE, may help to clarify a possible role of this enzyme in the assembly of amyloid-β-peptide into AD fibrils and plaques which colocalize with BuChE activity.[13] In this regard,

Inestrosa and colleagues[14] have described an involvement of a peripheral binding domain in AChE that is involved in binding with amyloid-β-peptide. Finally, **4j**, characterized by an optimally balanced inhibitory activity for both enzymes, may represent a lead structure to generate enzyme inhibitors as novel therapeutics for severe neurodegenerative diseases.

Experimental Procedures

Melting points were determined using an Electrothermal 8103 apparatus. IR spectra were taken with Perkin-Elmer 398 and FT 1600 spectrophotometers. ^{1}H NMR spectra were recorded on Bruker 200 MHz and Varian 500 MHz spectrometers with TMS as internal standard; the values of chemical shifts (δ) are given in ppm and coupling constants (J) in hertz (Hz). All reactions were carried out in an argon atmosphere. Flash chromatography purifications were performed by using Merck silica gel 230−400 mesh. GC−MS analyses were performed on a Saturn 3 (Varian) or Saturn 2000 (Varian) GC−MS system using a Chrompack DB5 capillary column (30 m × 0.25 mm i.d.; 0.25 μm film thickness). Mass spectra were recorded using a VG 70-250S spectrometer. Elemental analyses were performed on a Perkin-Elmer 240 °C elemental analyzer, and the results were within 0.4% of the theoretical values. Yields refer to purified products and are not optimized.

Bis[3-(*tert*-butoxycarbonylamino)propyl]-*N*-ethylamine (6a). To a solution of **5** (200.0 mg, 0.604 mmol) and K$_2$CO$_3$ (83.4 mg, 0.604 mmol) in dry CH$_3$CN (20.0 mL) was added iodoethane (48.3 μL, 0.604 mmol) slowly. The mixture was stirred at room temperature for 12 h. The solvent was evaporated, water was added, and the mixture was extracted with EtOAc. The organic layer was dried on Na$_2$SO$_4$ and evaporated, to provide **6a** as a clear oil: yield 50%; ^{1}H NMR (CD$_3$OD) δ 0.89 (t, 3H, J = 6.9 Hz), 1.32 (s, 18H), 1.42−1.64 (m, 4H), 2.30−2.37 (m, 2H), 2.53 (t, 4H, J = 6.4 Hz), 3.04− 3.10 (m, 4H). Anal. (C$_{18}$H$_{37}$N$_3$O$_4$) C, H, N.

Bis[3-(*tert*-butoxycarbonylamino)propyl]-*N*-allylamine (6b). Following the procedure described above for **6a** and using 3-bromopropene, **6b** was obtained as a clear oil: yield 47%; ^{1}H NMR (CDCl$_3$) δ 1.35 (s, 18H), 1.55−1.62 (m, 4H), 2.36 (t, 4H, J = 6.5 Hz), 2.94 (d, 2H, J = 6.6 Hz), 3.09 (q, 4H, J = 6.1 Hz), 5.02−5.11 (m, 2H), 5.24 (br s, 2H), 5.66−5.80 (m, 1H). Anal. (C$_{19}$H$_{37}$N$_3$O$_4$) C, H, N.

Bis[3-(*tert*-butoxycarbonylamino)propyl]-*N*-hydroxyethylamine (6c). Following the procedure described above for **6a** and using 2-bromoethanol, **6c** was obtained as a clear oil: yield 10%; ^{1}H NMR (CD$_3$OD) δ 1.41 (s, 18H), 1.62 (q, 4H, J = 6.8 Hz), 2.49−2.63 (m, 6H), 3.05 (t, 4H, J = 6.8 Hz), 3.60 (t, 2H, J = 6.0 Hz). Anal. (C$_{18}$H$_{37}$N$_3$O$_5$) C, H, N.

N,N-Bis[3-[(1,2,3,4-tetrahydroacridin-9-yl)amino]propyl]-N-ethylamine (4b). To a solution of **6a** (384.1 mg, 1.07 mmol) in dry CH$_2$Cl$_2$ (5.0 mL), CF$_3$COOH (3.0 mL) was added and the mixture was stirred for 1 h at room temperature. The resulting solution was concentrated in vacuo, and the crude residue was washed with ether. Then, triethylamine (TEA, 270.4 μL, 1.94 mmol), 9-chloro-1,2,3,4-tetrahydroacridine (421.0 mg, 1.94 mmol), and pentanol (5.0 mL) were added, and the mixture was heated to reflux (160 °C) for 12 h. After cooling to room temperature, the mixture was diluted with CH$_2$Cl$_2$ (50 mL) and then washed with 10% NaOH (1 × 50 mL) and water (2 × 40 mL). The organic layer was dried over Na$_2$SO$_4$, filtered, and concentrated in vacuo. Then purification by flash column chromatography (EtOAc/CH$_3$OH/TEA, 10:1:1) afforded **4b** as a yellow oil: yield 15%; ^{1}H NMR (CDCl$_3$) δ 1.02 (t, 3H, J = 7.1 Hz), 1.76−1.84 (m, 12H), 2.53−2.65 (m, 10H), 3.48− 3.55 (m, 4H), 4.16−4.22 (m, 4H), 7.21−7.29 (m, 2H), 7.46− 7.53 (m, 2H), 7.85−7.93 (m, 4H); MS *m/z* 521, 324, 310, 284, 239, 212 (100). Anal. (C$_{34}$H$_{43}$N$_5$) C, H, N.

N,N-Bis[3-[(1,2,3,4-tetrahydroacridin-9-yl)amino]propyl]-N-allylamine (4c). Starting from **6b** and using the same procedure described above for **4b**, after purification by flash chromatography (EtOAc/TEA, 9:1), **4c** was obtained as a clear oil: yield 10%; ^{1}H NMR (CDCl$_3$) δ 1.76−1.85 (m, 12H), 2.57

(t, 4H, J = 6.7 Hz), 2.60−2.67 (m, 4H), 2.95−3.03 (m, 4H), 3.12 (d, 2H, J = 6.0 Hz), 3.47−3.53 (m, 4H), 5.11−5.20 (m, 2H), 5.76−5.90 (m, 1H), 7.22−7.29 (m, 2H), 7.46−7.54 (m, 2H), 7.86−7.93 (m, 4H); MS *m/z* 533, 492, 336, 322, 296, 239, 225, 211, 197, 182 (100). Anal. (C$_{35}$H$_{43}$N$_5$) C, H, N.

N,N-Bis[3-[(1,2,3,4-tetrahydroacridin-9-yl)amino]propyl]-N-hydroxyethylamine (4d). Starting from **6c** and using the same procedure described above for **4b**, after purification by flash chromatography (EtOAc/MeOH/TEA 13:1:2), **4d** was obtained as a clear oil: yield 11%; ^{1}H NMR (CDCl$_3$) δ 1.73− 1.93 (m, 12H), 2.51−2.61 (m, 10H), 3.00−3.03 (m, 4H), 3.44 (t, 4H, J = 6.8 Hz), 3.57 (t, 2H, J = 5.6 Hz), 7.28 (t, 2H, J = 7.9 Hz), 7.50 (t, 2H, J = 8.2 Hz), 7.87 (d, 4H, J = 8.8 Hz); MS *m/z* 537, 494, 355, 340, 326, 282, 239, 225, 211 (100). Anal. (C$_{34}$H$_{43}$N$_5$O) C, H, N.

9-*p*-Toluenesulfonyl-*N*-(1,2,3,4-tetrahydroacridin-9-yl)-nonan-1-amine (8). A solution of **7** (635.0 mg, 3.205 mmol) in dry CH$_3$CN (60.0 mL) was added to powdered KOH (180.0 mg, 3.205 mmol) under argon. To the vigorously stirred mixture at room temperature was added 1,9-di-*p*-toluenesulfonylnonane (1.5 g 3.205 mmol). After stirring at room temperature for 12 h, the resulting mixture was poured into water and extracted with EtOAc (3 × 150 mL). The combined organic layers were dried over MgSO$_4$, filtered, concentrated in vacuo, and purified by flash column chromatography (EtOAc/hexane/TEA, 6:4:2) to afford **8** as a yellowish oil: yield 10%; ^{1}H NMR (CDCl$_3$) δ 1.10−1.22 (m, 10H), 1.58−1.62 (m, 4H), 1.87−1.94 (m, 4H), 2.42 (s, 3H), 2.61−2.65 (m, 2H), 3.00−3.05 (m, 2H), 3.40−3.44 (m, 2H), 3.99−4.03 (m, 2H), 7.27−7.32 (m, 3H), 7.51 (t, 1H J = 7.5 Hz), 7.76 (d, 2H J = 7.8 Hz), 7.85−7.95 (m, 3H). Anal. (C$_{29}$H$_{38}$N$_2$O$_3$S) C, H, N.

N-(1,2,3,4-Tetrahydroacridin-9-yl)-9-[(1,2,3,4-tetrahydro-9-yl)thio]nonan-1-amine (4h). A solution of 1,2,3,4-tetrahydro-9-thioacridine (70.0 mg, 0.325 mmol) in dry CH$_3$CN (10.0 mL) was added to powdered KOH (18.2 mg, 0.325 mmol) under argon. The mixture was vigorously stirred at room temperature, and a solution of **8** (160.0 mg, 0.325 mmol) in CH$_3$CN was added. Stirring continued at room temperature for 4 h, and then the reaction mixture was poured into water and extracted with EtOAc. The combined organic layers were dried over Na$_2$SO$_4$, filtered, and concentrated in vacuo; the residue, purified by flash chromatography (EtOAc/hexane/TEA, 6:4:2), afforded **4h** as a clear yellow oil: yield 38%; ^{1}H NMR (CDCl$_3$) δ 1.22−1.32 (m, 10 H), 1.47−1.64 (m, 4H), 1.85.1.95 (m, 8H), 2.70−2.81 (m, 4H), 3.05−3.23 (m, 6H), 3.44 (t, 2H, J = 7.2 Hz), 7.31 (t, 1H, J = 7.1 Hz), 7.45−7.64 (m, 3H), 7.87−8.00 (m, 3H), 8.46 (d, 1H, J = 8.0 Hz); ESI-MS *m/z* 538 [M + H]$^+$, 340, 323 (100), 309, 295, 281, 267, 253, 239, 225, 211, 198. Anal. (C$_{35}$H$_{43}$N$_3$S) C, H, N.

Methyl-[(1,2,3,4-tetrahydro-9-yl)acridine]carboxylate (10). To a solution of 1,2,3,4-tetrahydro-9-acridinecarboxylic acid (**9**) (0.50 g, 1.9 mmol) in CH$_3$OH (50.0 mL) at room temperature was added CH$_2$N$_2$ until a yellow persistent coloring developed. The reaction mixture was stirred for 2 h at room temperature and concentrated in vacuo to yield **10** as colorless prisms: yield 96%; mp 167−8 °C; ^{1}H NMR (CDCl$_3$) δ 1.82−1.92 (m, 4H), 2.87 (t, 2H, J = 6.0 Hz), 3.09 (t, 2H, J = 6.1 Hz), 3.98 (s, 3H), 7.40 (t, 1H, J = 7.6 Hz), 7.54−7.63 (m, 2H), 7.95 (d, 1H, J = 8.3 Hz). Anal. (C$_{15}$H$_{15}$NO$_2$) C, H, N.

1,2,3,4-Tetrahydro-9-acridinecarboxaldehyde (11). To a solution of **10** (2.60 g, 11.0 mmol) in dry toluene (25.0 mL) under N$_2$ at −78 °C was added DIBAL-H (24.0 mL, 0.024 mmol) in a period of 20 min. The reaction mixture was stirred at −78 °C for 2 h. Then dry CH$_3$OH (5 mL) and a 1 M solution of Rochelle salt (10 mL) were added. Stirring was continued for a further 2 h, and the mixture was then extracted with EtOAc. The organic layer was dried on Na$_2$SO$_4$, filtered, and concentrated in vacuo. After purification by flash column chromatography (EtOAc/hexane, 8:2), **11** was obtained as yellow prisms: yield 64%; mp 68−70 °C; ^{1}H NMR (CDCl$_3$) δ 1.96−2.00 (m, 4H), 3.16−3.30 (m, 4H), 7.51−7.70 (m, 2H), 8.02 (d, 1H, J = 8.5 Hz), 8.48 (d, 1H, J = 8.6 Hz), 10.97 (s, 1H). Anal. (C$_{14}$H$_{13}$NO) C, H, N.

8-(1,2,3,4-Tetrahydroacridin-9-yl)oct-7-enenitrile (12). To a suspension of 6-cyanohexyl-1-triphenylphosphonium bromide (0.814 g, 1.20 × 1.5 mmol) in dry THF at −78 °C was added *t*-BuOK (0.201 g, 1.20 × 1.5 mmol), and the mixture was stirred for 30 min. Then **11** (0.250 g, 1.20 mmol), dissolved in dry THF, was slowly added at −78 °C, and the reaction mixture was stirred at room temperature for 1 h. Thereafter, a solution of NH_4Cl was added and the reaction mixture was extracted with EtOAc. The organic layer was dried on Na_2SO_4, filtered, and concentrated in vacuo. Purification by flash column chromatography (EtOAc/hexane, 1:1) gave compound **12** as a yellow oil: yield 73%; ^{1}H NMR (CDCl$_3$) δ 1.26−1.47 (m, 4H), 1.67−1.94 (m, 8H), 2.12 (t, 2H, J = 6.5 Hz), 2.70−2.73 (m, 2H), 3.08 (t, 2H, J = 5.9 Hz), 5.97 (dt, 1H, J = 11.4, 7.4 Hz), 6.40 (d, 1H, J = 11.4 Hz), 7.35 (t, 1H, J = 7.8 Hz), 7.53 (t, 1H, J = 7.5 Hz), 7.77 (d, 1H, J = 8.2 Hz), 7.92 (d, 1H, J = 8.2 Hz). Anal. (C$_{21}$H$_{24}$N$_2$) C, H, N.

8-(1,2,3,4-Tetrahydroacridin-9-yl)-7-octenyl-1-amine (13). To a suspension of LiAlH$_4$ (35.0 mg, 0.92 mmol) in dry Et$_2$O (15.0 mL) was slowly added **12** (0.140 g, 0.46 mmol), dissolved in the same solvent, at 0 °C. The mixture was stirred at room temperature for 2 h. Then 20% NaOH and water were added succesively at 0 °C; the organic layer was decanted and separated, and the aqueous solution was washed twice with Et$_2$O. The organic layers were combined, dried over Na$_2$SO$_4$, filtered, and concentrated in vacuo, to afford **13** as a clear oil: yield 86%; ^{1}H NMR (CDCl$_3$) δ 1.05−1.15 (m, 4H), 1.21−1.45 (m, 4H), 1.62−1.74 (m, 2H), 1.81−1.99 (m, 4H), 2.53 (t, 2H, J = 6.9 Hz), 2.71−2.81 (m, 2H), 3.10 (t, 2H, J = 6.3 Hz), 5.65−6.09 (m, 1H), 6.42 (d, 1H, J = 11.4 Hz), 7.27−7.47 (m, 1H), 7.54 (t, 1H, J = 9.0 Hz), 7.80 (d, 1H, J = 9.0 Hz), 7.95 (d, 1H, J = 8.6 Hz). Anal. (C$_{21}$H$_{28}$N$_2$) C, H, N.

N-(1,2,3,4-Tetrahydroacridin-9-yl)-N-[8-(1,2,3,4-tetrahydroacridin-9-yl)oct-7-en-1-yl]amine (14). A mixture of **13** (100.0 mg, 0.325 mmol), 9-chloro-1,2,3,4-tetrahydroacridine (106.0 mg, 0.487 mmol), and 1-pentanol (5 mL) was heated to reflux (160 °C) for 12 h. After cooling to room temperature, the mixture was diluted with CH$_2$Cl$_2$ (50 mL) and then washed with 10% NaOH (1 × 50 mL) and water (2 × 40 mL). The organic layer was dried over Na$_2$SO$_4$, filtered, and concentrated in vacuo. Pure **14** was obtained by means of flash chromatography purification (EtOAc/hexane/TEA, 6:4:0.5): yield 35%; ^{1}H NMR (CDCl$_3$) δ 1.10−1.35 (m, 6H), 1.48−1.58 (m, 2H), 1.62−1.74 (m, 2H), 1.81−1.99 (m, 8H), 2.58−2.68 (m, 2H), 2.71−2.85 (m, 2H), 3.05−3.28 (m, 4H), 3.41 (t, 2H, J = 6.9 Hz), 5.95−6.09 (m, 1H), 6.42 (d, 1H, J = 11.4 Hz), 7.27−7.45 (m, 2H), 7.49−7.59 (m, 2H), 7.75−8.05 (m, 4H); MS *m/z* 489, 292, 264, 236, 222, 208, 197 (100), 180. Anal. (C$_{34}$H$_{39}$N$_3$) C, H, N.

N-(1,2,3,4-Tetrahydroacridin-9-yl)-N-[8-(1,2,3,4-tetrahydroacridin-9-yl)oct-1-yl]amine (4i). To a solution of **14** (40.0 mg, 0.080 mmol) in CH$_3$OH (20.0 mL) was added 10% Pd/C. The reaction mixture was hydrogenated at room temperature in a Parr apparatus at 40 psi for 4 h, then the catalyst was filtered off through Celite, and the solution, taken to dryness, afforded compound **4i** as a colorless oil: yield 92%; ^{1}H NMR (CDCl$_3$) δ 1.29−1.50 (m, 8H), 1.53−1.57 (m, 4H), 1.75−1.79 (m, 2H), 1.89−2.01 (m, 6H), 2.58−2.62 (m, 2H), 2.81−3.05 (m, 4H), 3.08−3.13 (m, 2H), 3.18−3.23 (m, 2H), 3.78 (t, 2H, J = 6.9 Hz), 7.29−7.48 (m, 2H), 7.52−7.68 (m, 2H), 7.92 (t, 2H, J = 8.2 Hz), 8.10 (d, 1H, J = 8.3 Hz), 8.29 (d, 1H, J = 8.3 Hz); ESI-MS *m/z* 492 [M+H]$^+$, 464, 294, 281, 267, 253, 225, 211, 199 (100). Anal. (C$_{34}$H$_{41}$N$_3$) C, H, N.

9-[(3-Bromopropyl)sulfanyl]-1,2,3,4-tetrahydroacridine (16a). A solution of **15** (0.800 g, 3.72 mmol) in dry CH$_3$CN (50.0 mL) was added to powdered KOH (0.208 g, 3.72 mmol) under argon. To the vigorously stirred mixture at room temperature was added 1,3-dibromopropane (378.0 μL, 3.72 mmol). After stirring at room temperature for 12 h, the resulting mixture was poured into water and extracted with EtOAc (3 × 100 mL). The combined organic layers were dried over MgSO$_4$, filtered, and concentrated in vacuo. After purification by means of flash chromatography (EtOAc/hexane, 7:3), **16a** was obtained as a yellow oil: yield 74%; ^{1}H NMR (CDCl$_3$) δ 1.88−1.98 (m, 6H), 2.90 (dt, 2H, J = 1.1, 6.8 Hz), 3.06−3.18 (m, 4H), 3.39 (dt, 2H, J = 1.3, 6.6 Hz), 7.46 (t, 1H, J = 8.0 Hz), 7.58 (t, 1H, J = 8.5 Hz), 7.94 (d, 1H, J = 8.0 Hz), 8.40 (d, 1H, J = 8.5 Hz). Anal. (C$_{16}$H$_{18}$BrNS) C, H, N.

9-[(4-Bromobutyl)sulfanyl]-1,2,3,4-tetrahydroacridine (16b). Starting from **15** and 1,4-dibromobutane, the title compound was obtained following the procedure described for **16a**. After purification by means of flash chromatography (EtOAc/hexane, 7:3), **16b** was obtained as a yellow oil: yield 65%; ^{1}H NMR (CDCl$_3$) δ 1.61−1.71 (m, 2H), 1.90−1.96 (m, 6H), 2.81 (t, 2H, J = 7.2 Hz), 3.09−3.22 (m, 4H), 3.31 (t, 2H, J = 6.6 Hz), 7.49−7.65 (m, 2H), 7.97 (d, 1H, J = 8.4 Hz), 8.43 (d, 1H, J = 7.9 Hz). Anal. (C$_{17}$H$_{20}$BrNS) C, H, N.

***tert*-Butyl-N-(3-{methyl[3-(1,2,3,4-tetrahydroacridin-9-ylsulfanyl)propyl]amino}propyl)carbamate (18a).** To a solution of **16a** (0.25 g, 0.744 mmol) and diisopropylethylamine (DIPEA) (96.0 mg, 0.744 mmol) in dry CH$_3$CN (5 mL) was added *tert*-butyl-N-(3-methylaminopropyl)carbamate (140.0 mg, 0.744 mmol), and the mixture was stirred at room temperature for 12 h. Thereafter, the reaction mixture, concentrated in vacuo, was diluted with water and extracted with EtOAc. The obtained crude residue, after purification by flash chromatography (EtOAc/hexane/TEA, 9:1:0.5), gave compound **18a** as a colorless oil: yield 57%; ^{1}H NMR (CDCl$_3$) δ 1.38 (s, 9 H), 1.48−1.67 (m, 4H), 1.88−1.92 (m, 4H), 2.04 (s, 3H), 2.25 (t, 2H, J = 6.7 Hz), 2.30 (t, 2H, J = 6.9 Hz), 2.80 (t, 2H, J = 7.0 Hz), 3.05−3.19 (m, 6H), 7.46−7.61 (m, 2H), 7.91−7.95 (m, 1H), 8.41−8.45 (m, 1H). Anal. (C$_{25}$H$_{37}$N$_3$O$_2$S) C, H, N.

***tert*-Butyl-N-(3-{methyl[4-(1,2,3,4-tetrahydroacridin-9-ylsulfanyl)butyl]amino}propyl)carbamate (18b).** Using the procedure described above for **18a** and starting from **16b**, the title compound was obtained as a clear oil after purification by flash column chromatography: yield 63%; ^{1}H NMR (CDCl$_3$) δ 1.39 (s, 9 H), 1.51−1.54 (m, 6H), 1.88−2.05 (m, 4H), 2.10 (s, 3H), 2.20−2.32 (m, 4H), 2.77−2.82 (m, 2H), 3.08−3.22 (m, 6H), 7.48−7.60 (m, 2H), 7.95 (d, 1H, J = 8.3 Hz), 8.45 (d, 1H, J = 8.8 Hz). Anal. (C$_{26}$H$_{39}$N$_3$O$_2$S) C, H, N.

N-Methyl-N′-(1,2,3,4-tetrahydroacridin-9-yl)-N-[3-(1,2,3,4-tetrahydroacridin-9-ylsulfanyl)propyl]-1,3-propanediamine (4j). Similarly to the procedure described for **4b** (CH$_3$CN as a solvent), the title compound was prepared starting from **18a**. Pure **4j** was obtained by means of flash chromatography (EtOAc/hexane/TEA, 8:2:1): yield 35%; ^{1}H NMR (CDCl$_3$) δ 1.65−1.76 (m, 4H), 1.82−1.92 (m, 8H), 2.15 (s, 3H), 2.41 (t, 4H, J = 6.5 Hz), 2.63 (t, 2H, J = 5.5 Hz), 2.81 (t, 2H, J = 7.0 Hz), 2.99−3.25 (m, 6H), 3.50 (t, 2H, J = 6.3 Hz), 7.24 (t, 1H, J = 7.5 Hz), 7.39−7.60 (m, 3H), 7.85−7.96 (m, 3H), 8.42 (d, 1H, J = 8.1 Hz); MS *m/z* 524, 311, 239, 225, 212, 197 (100), 182. Anal. (C$_{33}$H$_{40}$N$_4$S) C, H, N.

N-Methyl-N′-(1,2,3,4-tetrahydroacridin-9-yl)-N-[4-(1,2,3,4-tetrahydroacridin-9-ylsulfanyl)butyl]-1,3-propanediamine (4l). Similarly to the procedure described for **4b** (CH$_3$CN as a solvent), the title compound was prepared starting from **18b**. Pure **4l** was obtained by means of flash chromatography (EtOAc/hexane/TEA, 8:2:1): yield 35%; ^{1}H NMR (CDCl$_3$) δ 1.53−1.56 (m, 4H), 1.74−1.80 (m, 2H), 1.85−1.95 (m, 6H), 2.22 (s, 3H), 2.31 (t, 2H, J = 6.9 Hz), 2.48 (t, 2H, J = 6.0 Hz), 2.51−2.64 (m, 4H), 2.80 (t, 2H, J = 6.5 Hz), 3.08−3.20 (m, 6H), 3.63 (t, 2H, J = 6.0 Hz), 7.31 (d, 1H, J = 8.3 Hz), 7.43−7.64 (m, 3H), 7.92−7.98 (m, 3H), 8.44 (d, 1H, J = 8.5 Hz); MS *m/z* 538, 323, 313, 270, 238, 225, 212, 197 (100), 182. Anal. (C$_{34}$H$_{42}$N$_4$S) C, H, N.

***tert*-Butyl-N-(3-{[3-(1,2,3,4-tetrahydroacridin-9-ylsulfanyl)propyl]amino}propyl)carbamate. (17a).** Starting from **16a** and *tert*-butyl-N-(3-aminopropyl)carbamate, and following the procedure described for **18a**, the title compound was obtained as a clear oil after purification by flash column chromatography: yield 61%; ^{1}H NMR (CDCl$_3$) δ 1.36 (s, 9H), 1.48−1.68 (m, 4H), 1.85−1.91 (m, 4H), 2.51 (t, 2H, J = 6.3 Hz), 2.58 (t, 2H, J = 6.9 Hz), 2.81 (t, 2H, J = 7.5 Hz), 3.04−3.18 (m, 6H), 5.05 (br s, 1H), 7.41−7.59 (m, 2H), 7.89−7.94 (m, 1H), 8.39−8.43 (m, 1H). Anal. (C$_{24}$H$_{35}$N$_3$O$_2$S) C, H, N.

***tert*-Butyl-*N*-(3-{[4-(1,2,3,4-tetrahydroacridin-9-ylsulfanyl)butyl]amino}propyl)carbamate (17b).** Starting from **16b** and *tert*-butyl-*N*-(3-aminopropyl)carbamate, and following the procedure described for **18a**, the title compound was obtained as a clear oil after purification by flash column chromatography: yield 57%; ^{1}H NMR (CDCl$_3$) δ 1.35 (s, 9H), 1.46–1.58 (m, 6H), 1.85–1.92 (m, 4H), 2.40–2.48 (m, 2H), 2.52 (t, 2H, J = 6.4 Hz), 2.71–2.77 (m, 2H), 3.03–3.17 (m, 6H), 5.11 (br s, 1H), 7.43 (t, 1H, J = 7.1 Hz), 7.55 (t, 1H, J = 6.9 Hz), 7.91 (d, 1H, J = 8.9 Hz), 8.40 (dd, 1H, J = 1.2, 8.8 Hz). Anal. (C$_{25}$H$_{37}$N$_3$O$_2$S) C, H, N.

***tert*-Butyl-*N*-(3-{acetyl[3-(1,2,3,4-tetrahydroacridin-9-ylsulfanyl)propyl]amino}propyl)carbamate (19a).** To a solution of **17a** (388.0 mg, 0.906 mmol) and TEA (151.5 μL, 1.087 mmol) in dry CH$_2$Cl$_2$ (10.0 mL) at 0 °C, with stirring, was added acetyl chloride (77.3 μL, 1.087 mmol) slowly with stirring. The mixture was stirred at room temperature for 3 h. Water was added, and the mixture was extracted with CH$_2$Cl$_2$. The organic layer, dried on Na$_2$SO$_4$ and evaporated, gave **19a** as a colorless oil with quantitative yield; ^{1}H NMR (CDCl$_3$) δ 1.39 (s, 9H), 1.47–1.57 (m, 2H), 1.65–1.77 (m, 2H), 1.89–1.97 (m, 4H), 1.98 (s, 3H), 2.78 (t, 2H, J = 6.7 Hz), 2.96–3.03 (m, 2H), 3.08–3.18 (m, 4H), 3.22–3.32 (m, 4H), 5.23 (br s, 1H), 7.25–7.64 (m, 2H), 7.94–7.98 (m, 1H), 8.36–8.44 (m, 1H). Anal. (C$_{26}$H$_{37}$N$_3$O$_3$S) C, H, N.

***tert*-Butyl-*N*-(3-{acetyl[4-(1,2,3,4-tetrahydroacridin-9-ylsulfanyl)butyl]amino}propyl)carbamate (19b).** Starting from **17b** and following the procedure described for **19a**, the title compound was obtained as a clear oil in quantitative yield: ^{1}H NMR (CDCl$_3$) δ 1.35 (s, 9H), 1.42–1.57 (m, 6H), 1.82–1.90 (m, 4H), 1.94 (s, 3H), 2.70–2.75 (m, 4H), 2.91–3.13 (m, 6H), 3.22–3.28 (m, 2H), 7.44–7.59 (m, 2H), 7.89–7.93 (m, 1H), 8.36–8.40 (m, 1H). Anal. (C$_{27}$H$_{39}$N$_3$O$_3$S) C, H, N.

***N*-[3-(1,2,3,4-Tetrahydroacridin-9-ylamino)propyl]-*N′*-[3-(1,2,3,4-tetrahydroacridin-9-ylsulfanyl)propyl]acetamide (4k).** Using the same procedure described for **4b** (CH$_3$CN as a solvent), the title compound was obtained as a clear oil after purification by flash column chromatography (EtOAc/hexane/TEA, 9:1:0.5): ^{1}H NMR (CDCl$_3$) δ 1.67–1.79 (m, 4H), 1.91–2.07 (m, 8H), 2.15 (s, 3H), 2.74–2.84 (m, 4H), 3.06–3.25 (m, 6H), 3.29–3.38 (m, 6H), 7.30–7.33 (m, 1H), 7.45–7.57 (m, 3H), 7.95–8.01 (m, 3H), 8.38–8.48 (m, 1H); ESI-MS m/z 553 [M + H]$^+$, 356, 256, 239, 225, 211, 197 (100). Anal. (C$_{34}$H$_{40}$N$_4$OS) C, H, N.

***N*-[3-(1,2,3,4-Tetrahydroacridin-9-ylamino)propyl]-*N′*-[4-(1,2,3,4-tetrahydroacridin-9-ylsulfanyl)butyl]acetamide (4m).** Using the same procedure described for **4b** (CH$_3$CN as a solvent), the title compound was obtained as a clear oil after purification by flash column chromatography (EtOAc/hexane/TEA, 9:1:0.5): ^{1}H NMR (CDCl$_3$) δ 1.49–1.74 (m, 6H), 1.80–1.96 (m, 8H), 2.06 (s, 3H), 2.66–2.84 (m, 4H), 3.04–3.22 (m, 8H), 3.35–3.43 (m, 4H), 7.32–7.35 (m, 1H), 7.47–7.61 (m, 3H), 7.85–7.89 (m, 2H), 7.98 (t, 2H, J = 8.2 Hz), 8.43 (d, 1H, J = 8.3 Hz); MS m/z 566, 369, 270, 228, 182. Anal. (C$_{35}$H$_{42}$N$_4$OS) C, H, N.

Molecular Modeling. All molecular modeling studies were performed on SGI Indigo II R10000 and SGI Octane 2XR10000 workstations.

BuChE and AChE crystal structures were downloaded from the PDB data bank (http://www.rcsb.org/pdb/; PDB IDs: 1P0I, 1P0M, 1P0P, 1P0Q, and 1B41). Hydrogens were added to all the PDB structures considering a pH value of 7.2.

To introduce compounds into both hAChE (1B41) and hBuChE (1P0I) crystal structures, their ligands, fasciculin-2 and butyrylcholine hydrolysis products, respectively, were removed, by using the unmerge command in the Biopolymer module of Insight2000.1 (Accelrys, San Diego). An in-depth analysis of the conserved water molecules in the crystal structure of BuChE was performed (Insight2000.1 Homology module) to select those to include in subsequent calculations. On the basis of this inspection, all the water molecules present in 1P0I were maintained, with the exception of those that would sterically overlap with the ligand.

The newly designed compounds **4d**, **4e**, **4g**, **4k**, **4l**, and **4m** were built using the Insight 2000.1 Builder module. Tacrine moieties of all selected compounds and amine groups of **4d** and **4l** were considered protonated in all calculations performed, as a consequence of the estimation of apparent pK_a values calculated by using the ACD/pKa DB version 7.00 software (Advanced Chemistry Development Inc., Toronto, Canada). Partial charges of protonated compounds were manually assigned by comparing partial charges assigned by the CVFF force field[15] with those calculated by MNDO semiempirical 1 SCF calculations performed on the neutral and the ionized compounds.

Compounds **4d**, **4e**, **4g**, **4k**, **4l**, and **4m** were then subjected to conformational search. Due to the high flexibility of the structures under study, their conformational space was sampled through 100 cycles of simulated annealing (Tripos force field, Sybyl software, Tripos, San Louis), by using an already described general procedure.[11] Resulting structures were subjected to energy minimization within the Insight2000.1 Discover module (CVFF force field, conjugate gradient algorithm; $\epsilon = 80*r$) until the maximum RMS derivative was less than 0.001 kcal/Å, and subsequently ranked by their conformational energy values.

Since the flexible docking procedure formally requires a reasonable starting structure, ligands were oriented in the active site of the enzymes on the basis of previously reported results,[11] although in the subsequent flexible docking protocol all the systems were perturbed by means of Monte Carlo and simulated annealing procedures. A visual inspection of the low energy resulting conformers, placed in the 1P0I active sites, led to the selection of each starting ligand–protein complex. All subsequent structural calculations were performed using the CVFF force field.

Obtained complexes were subjected to preliminary energy minimization (steepest descent algorithm; $\epsilon = 1$) until the maximum RMS derivative was less than 0.5 kcal/Å, to generate roughly docked starting structures, as required by the Affinity docking procedure. Successively, flexible docking was achieved using the Affinity module in the Insight2000.1 suite, setting the SA Docking procedure,[16] and the Cell Multipole[17] method for nonbond interactions. A binding domain area was defined as a subset including the ligand and all the residues and water molecules having at least one atom within a 5 Å radius from any given ligand atom. All atoms included in the binding domain area were left free to move during the entire docking calculations. A Monte Carlo/minimization approach for random generation of a maximum of twenty structures was used, with an energy tolerance of 10^6 kcal/mol to ensure a wide variance of the input structures to be minimized (2500 iterations; $\epsilon = 1$). During this step the ligand is moved by a random combination of translation, rotation, and torsional changes (Flexible Ligand option, considering all rotatable bonds), to sample both the conformational space of the ligand and its orientation with respect to the enzyme. van der Waals (vdW) and Coulombic terms were scaled to a factor of 0.1 to avoid very severe divergences in the Coulombic and vdW energies. The Metropolis test, at a temperature of 310 K, and a structure similarity check (RMS tolerance = 0.3 kcal/Å) were applied to select acceptable structures. Fifty stages of simulated annealing (100 fs each) were applied on the resulting complexes. Over the course of the simulated annealing, system temperature was linearly decreased from 500 to 300 K; concurrently the van der Waals and Coulombic scale factors were similarly decreased from their initial values (defined above as 0.1) to their final value (1.0). A final round of 10^6 minimization steps was applied at the end of the molecular dynamics.

After the docking procedure, the resulting complexes needed to be further minimized (CVFF force field, $\epsilon = 1$) by a combination of steepest descent (maximum RMS derivative less than 0.1 kcal/Å) and conjugate gradient algorithms (maximum RMS derivative less than 0.01 kcal/Å).

The geometry of π–π interactions was evaluated considering[18–21] (i) the distance between the centroids of the

aromatic rings, (ii) the angle between the planes of the rings, (iii) the offset value, and (iv) the direction of the dipole vectors.

Measurement of FBSAChE/EqBuChE Inhibitory Activity. The biological activity of the new homo- and hetero-bivalent analogues of THA (THA-An) were evaluated using purified FBSAChE and EqBuChE. AChE and BuChE activities were measured in 50 mM sodium phosphate, pH 8.0, at 25 °C as described using acetylthiocholine (ATC) and butyrylthiocholine (BTC) as substrates, respectively.[4] Inhibition of enzyme activity was measured over a substrate concentration range of 0.01−30 mM and at least six inhibitor concentrations to determine the components of competitive and noncompetitive inhibition. Plots of initial velocities versus substrate concentrations at a series of inhibitor concentrations were analyzed by nonlinear least-squares methods to determine the values of K_m (Michaelis−Menten constant) and V_{max} (maximal velocity). Nonlinear regression analysis of the plots of V_{max}/K_m values versus [THA-An] was used for the determination of K_i values. The K_i values for the inhibition of FBSAChE and EqBuChE by the various inhibitors are reported in Table 1.

Experiments on Human Enzymes. Quantitation of Anticholinesterase Activity. The action of compounds to inhibit the ability of freshly prepared human AChE and BuChE to enzymatically degrade their respective specific substrates, acetyl(β-methyl)thiocholine and *s*-butyrylthiocholine (0.5 mmol/L) (Sigma Chemical Co., St. Louis, MO), was quantified. Specifically, samples of AChE and BuChE were derived from erythrocytes and plasma, respectively. Compounds were dissolved in Tween 80/EtOH 3:1 (v:v; <150 μL total volume) and were diluted in 0.1 M Na_3PO_4 buffer (pH 8.0) in half-log concentrations to provide a final concentration range that spanned 0.3 nM to 30 μM. Tween 80/EtOH was diluted in excess of 1 in 5000, and no inhibitory action on either AChE or BuChE was detected in a separate series of control experiments.

For the preparation of hBuChE, freshly collected human blood was centrifuged ($10000g$, 10 min, 4 °C) and plasma was removed and diluted 1:125 with 0.1 M Na_3PO_4 buffer (pH 7.4). For AChE preparation, whole red blood cells were washed five times in isotonic saline, lysed in 9 volumes of 0.1 M Na_3PO_4 buffer (pH 7.4) containing 0.5% Triton-X (Sigma), and then diluted with an additional 19 volumes of buffer to a final dilution of 1:200.

Analysis of anticholinesterase activity was undertaken by utilizing a 25 μL sample of each enzyme preparation, and was undertaken at their optimal working pH, 8.0, in 0.1 M Na_3PO_4 buffer (0.75 mL total volume). Compound or buffer alone was preincubated with enzyme (30 min, at room temperature), and then the samples were incubated with their respective substrates together with 5,5'-dithiobis-2-nitrobenzoic acid (0.5 mmol/L, 25 min, 37 °C). Substrate/enzyme interaction was immediately halted by the addition of excess enzyme inhibitor (physostigmine 1×10^{-5} M), and production of a yellow thionitrobenzoate anion was then measured by spectrophotometer at 412 nm wavelength. To correct for nonspecific substrate hydrolysis, aliquots were coincubated under conditions of absolute enzyme inhibition (by the addition of 1×10^{-5} M physostigmine), and the associated alteration in absorbance was subtracted from that observed through the concentration range of each test compound. Each agent was analyzed on four separate occasions and assayed alongside physostigmine, as a control and external standard whose activity is well documented. The enzyme activity at each concentration of test compound was expressed as a percent of the activity in the absence of compound. This was transformed into a logit format (logit = ln(% activity/100 minus % activity)) and then was plotted as a function of its log concentration. Inhibitory activity was calculated as an IC_{50}, defined as the concentration of compound (nM) required to inhibit 50% of enzymatic activity, and was determined from a correlation between log concentration and logit activity. Only results obtained from (i) correlation coefficients of $r^2 > -0.98$ and (ii) studies wherein the IC_{50} value of the external control, physostigmine, matched its documented activity (IC_{50} AChE 20 to 30 nM; BuChE 10 to 20

nM) were considered acceptable. Studies that did not obtain this threshold were repeated.

Supporting Information Available: Elemental analyses for title compounds. This material is available free of charge via the Internet at http://pubs.acs.org.

References

(1) Mesulam, M. Neuroanatomy of cholinesterases in the normal human brain and in Alzheimer's disease. In *Cholinesterase and cholinesterase inhibitors*; Giacobini, E., Ed.; Martin Donitz: London, 2000; pp 121−137.

(2) Giacobini, E. Cholinergic functions in Alzheimer's disease. *Int. J. Geriatr. Psychiatry* **2003**, *18*, S1−S5, and references therein.

(3) Gentry, M. K.; Doctor, B. P. In *Cholinesterases: structure, function, mechanism, genetics, and cell biology*; Massoulie, J., Bacou, F., Barnard, E. A., Chatonnet, A., Doctor, B. P., Eds.; American Chemical Society: Washington, DC, 1991; pp 394−398.

(4) Saxena, A.; Redman, A. M. G.; Jiang, X.; Lockridge, O.; Doctor, B. P. Differences in Active Site Gorge Dimension of Cholinesterases Revealed by Binding of Inhibitors to Human Butyrylcholinesterase. *Biochemistry* **1997**, *36*, 14642−14651.

(5) Mack, A.; Robitzki, A. The Key Role of Butyrylcholinesterase during neurogenesis and neural disorders: an antisense-5′-butyrylcholinesterase-DNA study. *Prog. Neurobiol.* **2000**, *60*, 607−628 and references therein.

(6) Greig, N. H.; Utsuki, T.; Yu, Q.-S.; Zhu, X.; Holloway, H. W.; Perry, T.; Lee, B.; Ingram, D. K.; Lahiri, D. K. A new therapeutic target in Alzheimer's disease treatment: attention to butyrylcholinesterase. *Curr. Med. Res. Opin.* **2001**, *17*, 1−6.

(7) Mesulam, M. M.; Guillozet, A.; Shaw, P.; Levey, A.; Duysen, E. G.; Lockridge, O. Acetylcholinesterase knockouts establish central cholinergic pathways and can use butyrylcholinesterase to hydrolyse acetylcholine. *Neuroscience* **2002**, *110*, 627−639.

(8) Yu, Q.-S.; Holloway, H. W.; Utsuki, T.; Brossi, A.; Greig, N. H. Synthesis of novel phenserine-based-selective inhibitors of butyrylcholinesterase for Alzheimer's disease. *J. Med. Chem.* **1999**, *42*, 1855−1861.

(9) Giacobini, E.; Spiegel, R.; Enz, A.; Veroff, A. E.; Cutler, N. R. Inhibition of acetyl- and butyryl-cholinesterase in the cerebrospinal fluid of patients with Alzheimer's disease by rivastigmine: correlation with cognitive benefit. *J. Neural Transm.* **2002**, *109*, 1053−1065.

(10) Savini, L.; Campiani, G.; Gaeta, A.; Pellerano, C.; Fattorusso, C.; Chiasserini, L.; Fedorko, J. M.; Saxena, A. Novel and potent tacrine-related hetero- and homobivalent ligands for acetylcholinesterase and butyrylcholinesterase. *Bioorg. Med. Chem. Lett.* **2001**, *11*, 1779−1782.

(11) Savini, L.; Gaeta, A.; Fattorusso, C.; Catalanotti, B.; Campiani, G.; Chiasserini, L.; Pellerano, C.; Novellino, E.; McKissic, D.; Saxena, A. Specific Targeting of Acetylcholinesterase and Butyrylcholinesterase Recognition Sites. Rational Design of Novel, Selective, and Highly Potent Cholinesterase Inhibitors. *J. Med. Chem.* **2003**, *46*, 1−4.

(12) Carlier, P. R.; Chow, E. S.-H.; Han, Y.; Liu, J.; El Yazal, J.; Pang, Y.-P. Heterodimeric tacrine-based acetylcholinesterase inhibitors: investigating ligand-peripheral site interactions. *J. Med. Chem.* **1999**, *42*, 4225−4231 and references therein.

(13) Geula, C.; Mesulam, M. M. Cholinesterases and the pathology of Alzheimer disease. *Alzheimer Dis. Assoc. Disord.* **1995**, *9* (Suppl. 2), 23−28.

(14) De Ferrari, G. V.; Canales, M. A.; Shin, I.; Weiner, L. M.; Silman, I.; Inestrosa, N. C. A structural motif of acetylcholinesterase that promotes amyloid β-peptide fibril formation. *Biochemistry* **2001**, *40*, 10447−10457.

(15) Dauber-Osguthorpe, P.; Roberts, V. A.; Osguthorpe, D. J.; Wolff, J.; Genest, M.; Hagler, A. T. Structure and energetics of ligand binding to proteins: E. coli dihydrofolate reductase-trimethoprim, a drug-receptor system. *Proteins* **1988**, *4*, 31−47.

(16) Senderowitz, H.; Guarnieri, F.; Still, W. C. A Smart Monte Carlo Technique for Free Energy Simulations of Multiconformational Molecules. Direct Calculations of the Conformational Populations of Organic Molecules. *J. Am. Chem. Soc.* **1995**, *117*, 8211−8219.

(17) Ding, H. Q.; Karasawa, N.; Goddard, W. A., III. Atomic level simulations on a million particles: The cell multipole method for Coulomb and London non-bond interactions. *J. Chem. Phys.* **1992**, *97*, 4309−4315.

(18) Singh, J.; Thornton, J. M. SIRIUS. An automated method for the analysis of the preferred packing arrangements between protein groups. *J. Mol. Biol.* **1990**, *211*, 595−615.

(19) Hunter, C. A.; Lawson, K. R.; Perkins, J.; Urch, C. J. Aromatic interactions. *J. Chem. Soc., Perkin Trans. 1* **2001**, *2*, 651−669.

(20) Cubero, E.; Luque, J. F.; Orozco, M. Is polarization important in cation-π interactions? *Proc. Natl. Acad. Sci. U.S.A.* **1998**, *95*, 5976−5980.

(21) Kim, K. S.; Tarakeshwar, P.; Yong Lee, J. Molecular clusters of π-Systems: Theoretical Studies of Structures, Spectra, and Origin of Interaction Energies. *Chem. Rev.* **2000**, *100*, 4145−4185.